CONTRIBUTION FROM THE CHEMISTRY DEPARTMENTS, UNIVERSITY OF WYOMING, LARAMIE, WYOMING 82070, AND POLYTECHNIC INSTITUTE OF BROOKLYN, BROOKLYN, NEW YORK 11201

The Electronic Structures of Cr(V) and Mn(V) in Phosphate and Vanadate Hosts

BY J. B. MILSTEIN,[1a] J. ACKERMAN, S. L. HOLT,*[1b] AND B. R. MCGARVEY[1c]

Received August 5, 1971

The optical absorption spectra of Mn^{5+} and Cr^{5+} in Sr_2VO_4Cl, Li_3PO_4, Ca_2PO_4Cl, and Ca_2VO_4Cl are reported and interpreted in light of current theories.

Introduction

Recently, much attention has been focused upon obtaining a description of the electronic structures of tetrahedral oxyanions which contain Cr(V)[2-4] and Mn(V).[5-7]

This work has included a determination of the ground state of Cr(V) in $Ca_2(PO_4,CrO_4)Cl$,[2] the determination of the structure of Ca_2CrO_4Cl,[8] and investigation of the excited state of Mn(V) and Cr(V)[3,4] in Ca_2PO_4Cl using electronic absorption spectroscopy. In addition, mention has been made of preliminary work on the electron spin resonance spectrum of $Ca_2(PO_4,MnO_4)Cl$. Several problems remain to be solved, however, before one can be completely satisfied with the description of the electronic structure suggested by this earlier work. Among these are: (1) the effect of lattice anion site size upon the absorption spectra, (2) the possible presence of a Jahn–Teller distortion for Cr(V), and (3) the surprising prominence of a ν_4 excited-state vibration, evidenced in the vibrational structure observed in the absorption spectrum of $[CrO_4]^{3-}$.

Experimental Section

Preparation of $Sr_2(VO_4,CrO_4)Cl$ and $Sr_2(VO_4,MnO_4)Cl$.—Anhydrous $SrCl_2$ (25–30 g), V_2O_5 (2 g), and MnO_2 (0.01–0.1 g) were mixed and fired in air at 1000° for 1–2 hr. The resulting molten mixture was cooled at approximately 4°/hr to 200–300°. The crystals, which are blue, with varying intensity depending upon the amount of manganese present in the melt, were then leached from the excess solidified flux with water. The predominant crystal habit was that of a hexagonal platelet.

The Cr(V)-containing species was prepared in a similar fashion with the addition of Cr_2O_3 in place of MnO_2. The crystal habit of $Sr_2(VO_4,CrO_4)Cl$ was the same as the above but the crystals displayed a green coloration.

Preparation of $Ca_2(VO_4,CrO_4)Cl$.—The preparation of this species was similar to the preparation of the strontium analog with the exception that anydrous $CaCl_2$ was used in place of the $SrCl_2$.

Preparation of $Li_3(PO_4,MnO_4)$ and $Li_3(PO_4,CrO_4)$.—A mixture of LiCl (25–30 g), Li_3PO_4 (0.5–1.0 g), and MnO_2 (0.01–0.1 g) or CrO_3 (0.01–0.1 g) was heated at 1000° in air for several hours and then cooled at 4°/hr to 200–300°. The crystals (displaying a chunky, blocklike habit) were collected after leaching the mixture with water. The Cr(V)-containing compound was green and the Mn(V)-containing crystals were blue.

Preparation of $Ca_2(PO_4,MnO_4)Cl$.—The preparation of this compound was identical with that reported earlier.[6,7]

Measurements of the Electronic Spectrum.—Optical measurements were conducted at 300, 80, and ~5°K by methods previously described.[6,9,10]

Measurements of the Electron Spin Resonance Spectrum.—Measurements were made at 77°K on a single crystal of $Ca_2(PO_4,MnO_4)Cl$ mounted with the *b* and *c* axes as rotation axes in a two-part experiment. The experimental frequency used was 9202.7 Mc/sec.

For each part of the experiment, the crystal was mounted on the end of a polypropylene plug with Duco cement. The plug was in turn placed on the end of the usual quartz esr tube. The orientation of the crystal was checked by single-crystal X-ray techniques and was found to be within two degrees of alignment with the rotation axis of the quartz tube in both cases. The crystal was rotated by 10° increments through 180°, and the esr signal was recorded for each such disposition with regard to the stationary magnetic field.

Crystal Structures

Ca_2VO_4Cl.—Banks, *et al.*,[11] have reported the structure of Ca_2VO_4Cl. This compound is isomorphous with Ca_2PO_4Cl belonging to the orthorhombic crystal class *Pbcm*. The site symmetry of the VO_4^{3-} ion is C_2, the only crystallographic symmetry element present being a twofold rotation axis perpendicular to the (100) crystal face. The habit of the $Ca_2(VO_4,MO_4)Cl$ crystals obtained from the molten salt reaction was with the (001) face predominant. As described earlier[3] polarized measurements made on the (001) crystal face indicate that the electronic transitions are best described as being quantized about an axis nearly collinear with the C_2 axis.

Sr_2VO_4Cl.—Nath and Hummel[5] have reported the preparation of microcrystalline Sr_2VO_4Cl. This material belongs to the same crystal class as Ca_2PO_4Cl and appears from its powder X-ray data to be isomorphous with Ca_2PO_4Cl. The crystals of $Sr_2(VO_4,MO_4)Cl$ grown in the present work display the same habit and cell dimensions similar to those noted for Ca_2PO_4Cl and Ca_2VO_4Cl.

Lithium Phosphate.—The structure of the high-temperature form of Li_3PO_4 has been determined by Zemann,[12] who prepared his samples by crystallization of Li_3PO_4 from molten LiCl, as we have done. Zemann determined the PO_4^{3-} ion in this structure to be tetrahedral with P–O bond distances of 1.55–1.56 (±0.02) Å and O–P–O bond angles of 109–110°. Powder patterns of the mixed $Li_3(PO_4,MO_4)$ compounds prepared

(1) (a) Abstracted in part from a thesis submitted to the Polytechnic Institute of Brooklyn in partial fulfillment of the degree of Doctor of Philosophy (Chemistry), June 1971. (b) Author to whom correspondence should be addressed at the University of Wyoming. (c) Polytechnic Institute of Brooklyn.

(2) E. Banks, M. Greenblatt, and B. R. McGarvey, *J. Chem. Phys.*, **47**, 3772 (1967).

(3) E. Banks, M. Greenblatt, and S. L. Holt, *ibid.*, **49**, 1431 (1968).

(4) C. Simo, E. Banks, and S. L. Holt, *Inorg. Chem.*, **9**, 183 (1970).

(5) D. K. Nath and F. A. Hummel, *J. Amer. Ceram. Soc.*, **52**, 8 (1969).

(6) J. Milstein and S. L. Holt, *Inorg. Chem.*, **8**, 1021 (1969).

(7) J. D. Kingsley, J. S. Prener, and B. Segall, *Phys. Rev. A*, **137**, 189 (1965).

(8) M. Greenblatt, E. Banks, and B. Post, *Acta Crystallogr.*, **23**, 166 (1967).

(9) S. L. Holt and A. Wold, *Inorg. Chem.*, **6**, 1594 (1967).

(10) C. Simo and S. L. Holt, *ibid.*, **7**, 2655 (1968).

(11) E. Banks, M. Greenblatt, and B. Post, *ibid.*, **9**, 2259 (1970).

(12) J. Zemann, *Acta Crystallogr.*, **13**, 863 (1960).

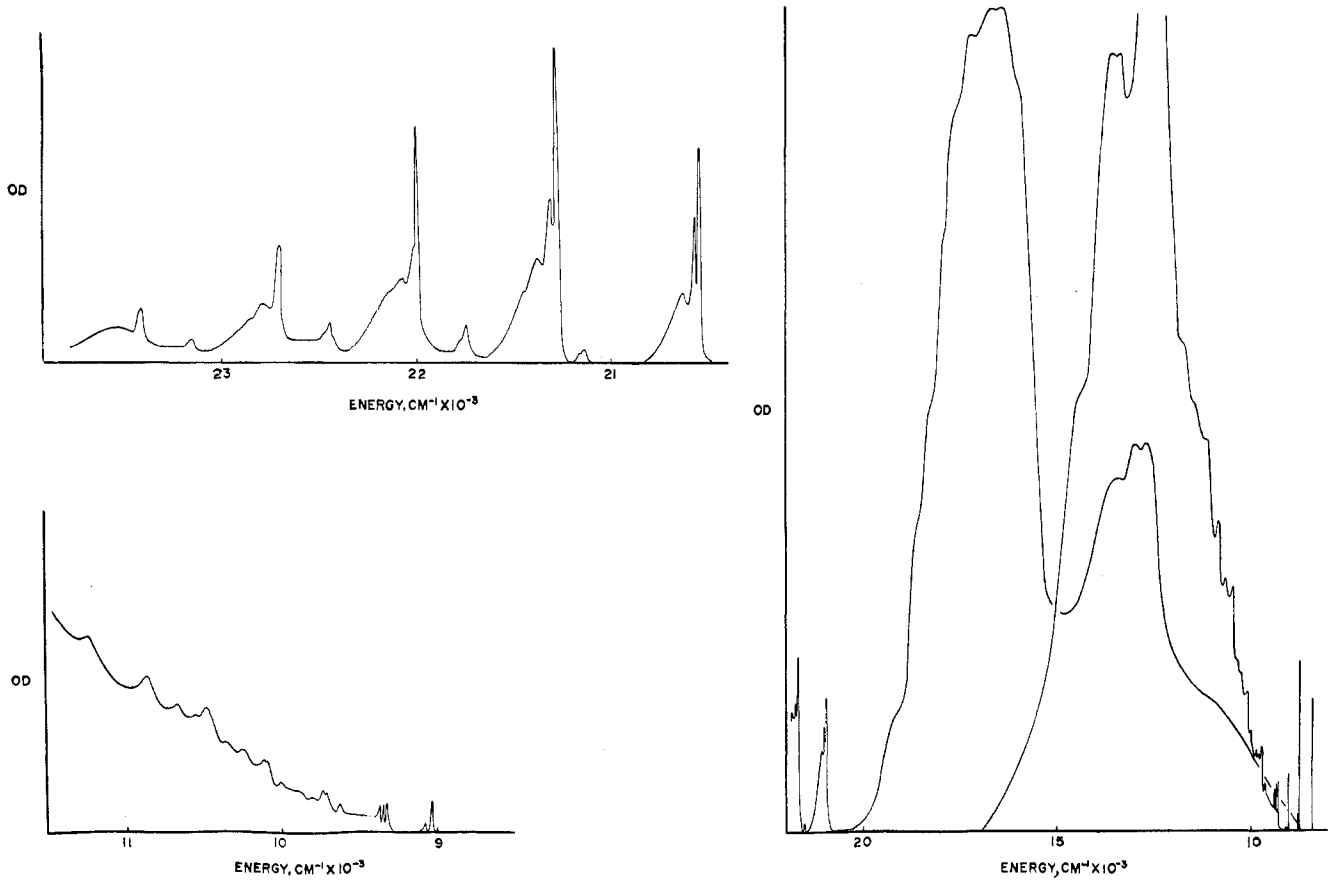

Figure 1.—The 5°K electronic absorption spectrum of $Sr_2(VO_4,MnO_4)Cl$.

in this work indicate that the Li_3PO_4 is the high-temperature form.

Results

$Sr_2(VO_4,MnO_4)Cl$.—The 5°K polarized spectrum of MnO_4^{3-} in Sr_2VO_4Cl is shown in Figure 1. This spectrum is seen to consist of five separate and distinct areas of absorption: (1) the two weak "lines" which appear at ~8500 cm^{-1} both with $\vec{E}||$ and $\vec{E}\perp$ to the molecular C_2 axis, (2) the area of broad intense absorption which occurs between 10,000 and 20,000 cm^{-1} and exhibits two major maxima with $\vec{E}\perp Z$ but only one with $\vec{E}||Z$, (3) a progression of five relatively sharp origins beginning at ~21,000 cm^{-1} which appear only when $\vec{E}\perp Z$, (4) the very intense maxima at ~32,000 cm^{-1}, and (5) a hiterto unreported set of sharp maxima commencing at ~9000 cm^{-1}. The band maxima are tabulated in Table I. The vibrational structure associated with the broad maxima in the 8000–20,000-cm^{-1} region is tabulated in Table II while that which accompanies the weak maxima in the 20,000–24,000-cm^{-1} region is given in Table III.

TABLE I
THE ELECTRONIC SPECTRUM OF MnO_4^{3-}

$Sr_2(VO_4,MnO_4)Cl$	
E, cm^{-1}	Assignment
9,000–11,000	$^3A_2(t_1^6e^2) \rightarrow {}^3T_2(t_1^6e^1t_2^1)$
11,000–15,000	$\rightarrow {}^3T_1(t_1^5e^3)$
15,000–19,000	$\rightarrow {}^3T_1(t_1^6e^1t_2^1)$
	$\rightarrow {}^3T_2(t_1^5e^3)$
$Li_3(PO_4,MnO_4)$	
E, cm^{-1}	Assignment
9,000–12,000	$^3A_2(t_1^6e^2) \rightarrow {}^3T_2(t_1^6e^1t_2^1)$
12,000–17,000	$\rightarrow {}^3T_1(t_1^5e^3)$
~33,000	$\rightarrow {}^3T_1(t_1^6e^1t_2^1)$
	$\rightarrow {}^3T_1(t_1^5e^2t_2^1)$

TABLE II
VIBRATIONAL STRUCTURE IN THE 8000–20,000-Cm^{-1} REGION OF THE $Sr(VO_4,MnO_4)Cl$ SPECTRUM

$\vec{E}\|\|Z$, cm^{-1}	Assignment	$\vec{E}\|\|Z$, cm^{-1}	Assignment
9,029	?	10,373	...
9,067	Unresolved	10,483	...
9,325	$^3B_2$	10,549	...
9,350	$+ \nu_5$	10,667	...
9,372	$+ 2\nu_5$	10,857	...
9,629	?	11,236	...
9,715	$+ \nu_4$	$\vec{E}\perp Z$, cm^{-1}	Assignment
9,732	$+ \nu_4 + \nu_5$	16,155	^3E
9,795	$+ \nu_4 + 2\nu_5$	16,529	$+ \nu_4$
9,872	...	16,863	$+ 2\nu_4$
10,010	...	17,621	$+ 3\nu_4$
10,086	$+ 2\nu_4$	17,986	$+ 4\nu_4$
10,106	...	18,369	$+ 5\nu_4$
10,262	...	18,762	$+ 6\nu_4$
		19,157	

$Li_3(PO_4,MnO_4)$.—The spectrum of hypomanganate-doped Li_3PO_4 was recorded with the incident radiation polarized parallel to all three crystallographic axes at room and liquid nitrogen temperature and with radiation polarized parallel to the crystallographic b and c axes at liquid helium temperature. No polarization behavior was observed.

The spectrum of MnO_4^{3-} in Li_3PO_4 at ~5°K is presented in Figure 2. At room temperature the spectrum that one observes for this system is virtually identical with that reported by Johnson, *et al.*,[13] and Kingsley,

(13) P. D. Johnson, J. S. Prener, and J. D. Kingsley, *Science*, **141**, 1179 (1963).

TABLE III
VIBRATIONAL STRUCTURE IN THE 20,000–24,000-CM^{-1} REGION OF THE $Sr_2(VO_4,MnO_4)Cl$ SPECTRUM

$\vec{E}\perp Z$, cm^{-1}	Assignment[a]	$\vec{E}\perp Z$, cm^{-1}	Assignment[a]
20,542	^1E	22,095	$^1E + 2\nu_1 + \nu_6$
20,563	$+ \nu_5$	22,158	$+ 2\nu_1 + \nu_7$
20,636	$+ \nu_6$	22,447	$+ 2\nu_1 + \nu_4$
20,700	$+ \nu_7$	22,701	$+ 3\nu_1$
21,039	$+ \nu_4$	22,779	$+ 3\nu_1 + ?$
21,290	$+ \nu_1$	22,873	$+ 3\nu_1 + \nu_7$
21,313	$+ \nu_1 + \nu_5$	22 936	$+ 3\nu_1 + ?$
21,386	$+ \nu_1 + \nu_6$	23,148	$+ 3\nu_1 + ?$
21,450	$+ \nu_1 + \nu_7$	23,403	$+ 4\nu_1$
21,749	$+ \nu_1 + \nu_4$	23,474	$+ 4\nu_1 + ?$
21,997	$+ 2\nu_1$	23,552	$+ 4\nu_1 + \nu_7$
22,022	$+ 2\nu_1 + \nu_5$	24,390	Unresolved

[a] $\nu_1 \simeq 750$ cm^{-1}, $\nu_4 \simeq 375$ cm^{-1}, $\nu_5 \simeq 25$ cm^{-1}, $\nu_6 \simeq 100$ cm^{-1}, $\nu_7 \simeq 150$ cm^{-1}.

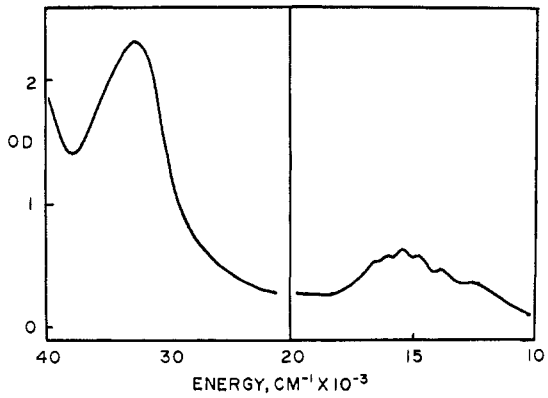

Figure 2.—The 5°K electronic absorption spectrum of $Li_3(PO_4,MnO_4)$.

et al.,[7] for a solution of MnO_4^{3-} in 12 *M* aqueous NaOH where the ion is expected to be tetrahedral. The 5°K spectrum is notable in its simplicity when compared to the spectrum of MnO_4^{3-} in $Sr_2(VO_4)Cl$. Indeed, neither the sharp lines in the near-infrared region, observed for both $Sr_2(VO_4,MnO_4)Cl$ and $Ca_2(PO_4,MnO_4)Cl$,[6,7] nor the series of five sharp maxima in the 21,000-cm^{-1} region was found to be present in the $Li_3(PO_4,MnO_4)$ spectrum. Absorption maxima are tabulated in Table I.

$Ca_2(VO_4,CrO_4)Cl$ and $Sr_2(VO_4,CrO_4)Cl$.—The spectrum of CrO_4^{3-}-doped into crystals of Ca_2VO_4Cl and Sr_2VO_4Cl was recorded at ~5°K. In both of these hosts one observes relatively sharp absorption maxima with $\vec{E}||Z$ and $\vec{E}\perp Z$ in the 10,000–14,000-cm^{-1} region, a broad band at 17,000 cm^{-1} which is present only when $\vec{E}\perp Z$, and maxima at ~27,000 cm^{-1} in both polarizations. Thus the overall spectrum of CrO_4^{3-} in these hosts is similar to that reported for $Ca_2(PO_4,CrO_4)Cl$[3,4] but does differ significantly in the structure observed on the lowest energy manifold. As the spectra of CrO_4^{3-} in the two vanadate hosts are virtually identical, only the lowest energy band in the $Ca_2(VO_4,CrO_4)Cl$ spectrum is shown, Figure 3. Manifold maxima with assignments are tabulated in Table IV. Table V contains a tabulation of the vibrational fine structure observed on the low-energy manifold.

$Li_3(PO_4,CrO_4)$.—The absorption spectrum of CrO_4^{3-} in the high-temperature form of Li_3PO_4 has been recorded at room temperature and liquid nitrogen temperature with incident radiation polarized along all three crystallographic axes and at ~5°K with the incident radiation polarized parallel to the *a* and *c* crystallographic axes. The last result is presented in Figure 4, where the solid line is the spectrum observed with $\vec{E}||c$ and the broken line for $\vec{E}||a$. The $\vec{E}||c$ polarization is the unique spectrum in this system, the *a* and *b* polariza-

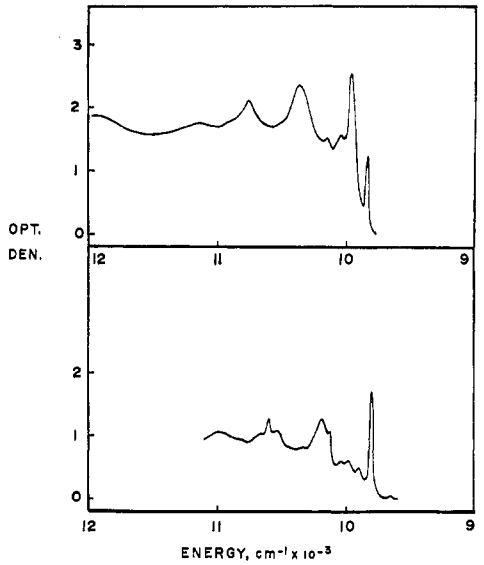

Figure 3.—The 10,000–14,000-cm^{-1} region of the spectrum of $Ca_2(VO_4,CrO_4)Cl$, at 5°K.

TABLE IV
THE ASSIGNMENT OF THE ELECTRONIC SPECTRUM OF CrO_4^{3-}

$Ca_2(VO_4,CrO_4)Cl$	
E, cm^{-1}	Assignment
9,500–14,000	$^2E(t_1^6e^1) \rightarrow {}^2T_2(t_1^6t_2^1)$
16,000–18,000	$\rightarrow {}^2T_2(t_1^5e^2)$
24,000–27,000	$\rightarrow {}^2T_2(t_1^5e^2)$
$Li_3(PO_4,CrO_4)$	
E, cm^{-1}	Assignment
10,000–16,000	$^2E(t_1^6e^1) \rightarrow {}^2T_2(t_1^6t_2^1)$
22,000–32,000	$\rightarrow {}^2T_1(t^5e^2)$
32,000–40,000	$\rightarrow {}^2T_2(t_1^5e^2)$

TABLE V
VIBRATIONAL STRUCTURE ON THE 10,000–14,000-CM^{-1} MANIFOLD OF $Ca_2(VO_4,CrO_4)Cl$

$\vec{E}\|\|Z$, cm^{-1}			$\vec{E}\perp Z$, cm^{-1}		
9,825	10,152	10,752	9,660	10,040	10,600
9,950	10,352	10,869	9,810	10,131	10,672
10,050	10,470	11,160	9,900	10,183	10,989
			9,970	10,526	

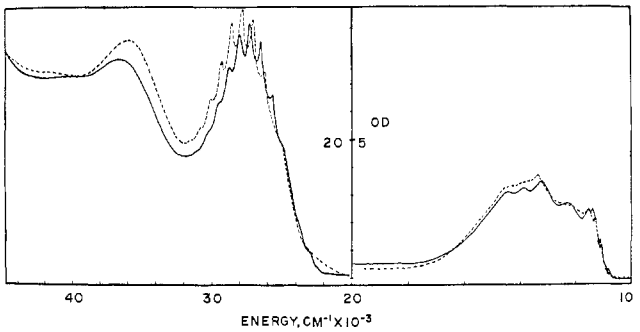

Figure 4.—The 5°K electronic absorption spectrum of $Li_3(PO_4,CrO_4)$.

tions being identical. A tabulation of the vibrational components in the spectrum of $Li_3(PO_4,CrO_4)$ is given in Table VI. An assignment of the major maxima is given in Table IV.

TABLE VI
VIBRATIONAL STRUCTURE IN THE 10,000–14,000- AND 21,000–30,000-Cm^{-1} REGIONS OF THE $Li_3(PO_4,Cr_4)$ SPECTRUM

$\vec{E}\|\|a$	$\vec{E}\|\|c$	$\vec{E}\|\|a$	ΔE
10,823	10,782	26,247	707
11,136	11,111	26,954	709
11,306	11,429	27,663	827
11,455	11,561	28,490	750
11,587	11,933	29,240	790
11,710	12,195	30,030	739
12,107	12,392	30,769	
12,270	12,747		
12,438	12,953		
12,755	13,228		
12,895	13,477		
13,089	13,889		
13,423	14,124		
14,104	14,493		
14,837			
15,456			
16,129			

$Ca_2(PO_4,MnO_4)Cl$.—Only one nuclide is present in natural manganese, namely ^{55}Mn. This nucleus exhibits a nuclear spin of $I = {}^5/_2$ which leads one to expect an esr signal consisting of 6 hyperfine lines to be observed for each magnetic site in the unit cell. Banks, *et al.*,[2] have shown that the four phosphate sites in Ca_2PO_4Cl exist in two magnetically equivalent pairs. Hence, one would expect to observe, at most, 12 hyperfine lines and fewer if accidental degeneracies happen to occur.

Our experimental results are not as simple as the above discussion would suggest. We have observed a more complicated signal in which the relative and absolute intensities, the line positions, and the number of lines present vary markedly.

For the part of the experiment in which the *b* axis was nearly coincident with the rotation axis, when the *a* axis was oriented along the magnetic field direction, a simple 6-line pattern was recorded, while with the *c* axis along the magnetic field, an exceedingly weak and poorly resolved signal, consisting of at least 9 lines, was observed. At intermediate angular orientations, rather complex signals consisting of as many as 22 lines, which vary in intensity and position with the angle of rotation, were seen. The 22-line pattern appears to be composed of two 6-line groups of roughly equal intensity, with weaker signals consisting of 5 lines superimposed on each 6 line pattern but spaced evenly between the individual components of the latter. Such a pattern is shown in Figure 5, with the lower field portion being better resolved than that to higher field.

When the *c* axis nearly coincided with the rotation axis and the *a* axis was aligned with the magnetic field, the simple 6-line pattern was again seen.

The spectrum became very weak and exceedingly complex when coincidence of the *b* axis and magnetic field direction occurred, as was also seen earlier in the case of the *c* axis. Again, for angular orientations between the *a* and *c* axes, fairly complex signals were recorded.

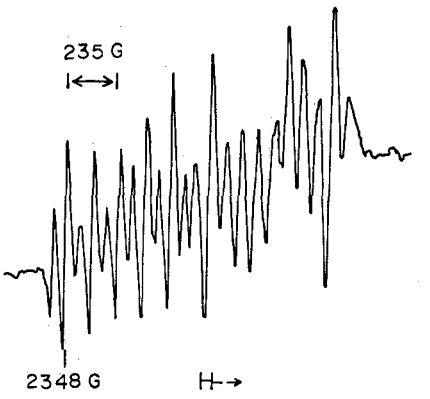

Figure 5.—The 80°K electron spin resonance spectrum of $Ca_2(PO_4,MnO_4)Cl$.

Discussion

The Electronic Structure of MnO_4^{3-}. The Optical Spectrum of $Sr_2(VO_4,MnO_4)Cl$.—The spectrum of $Sr_2(VO_4,MnO_4)Cl$, Figure 1, is highly reminiscent of that reported for $Ca_2(PO_4,MnO_4)Cl$[6,7] with the exception that a series of very weak maxima, in the polarization with $\vec{E}\|\|Z$ commencing at ~9000 cm^{-1}, is observed in this spectrum. (A reinvestigation of $Ca_2(PO_4,MnO_4)Cl$ reveals that in very thick or more highly doped crystals a similar series of maxima is observed.) This result is highly significant with regard to an accurate assignment of the electronic spectrum of MnO_4^{3-}. Earlier work on $Ca_2(PO_4,MnO_4)Cl$ led to the following assignment[6]

Energy, cm^{-1}	State transition	Orbital transition
10,000–15,000	$^3A_2 \rightarrow {}^3T_2$	$(t_1^6e^2) \rightarrow (t_1^6e^1t_2^1)$
	$^3A_2 \rightarrow {}^3T_1$	$\rightarrow (t_1^6e^1t_2^1)$
	$^3A_2 \rightarrow {}^3T_1$	$\rightarrow (t_1^5e^3)$
17,500	$^3A_2 \rightarrow {}^3T_2$	$\rightarrow (t_1^5e^3)$

This assignment may now be clarified and expanded.

Nath and Hummel[5] have shown that Sr_2VO_4Cl is isomorphous with Ca_2PO_4Cl. This requires the VO_4^{3-} site to possess C_2 symmetry. The electronic states in this symmetry have representations A or B with each of the T_1 and T_2 states yielding one state of A and two states of B symmetry. The A_2 ground state yields and correlates with the A representation in this lower symmetry. The selection rules are then A → A ($\vec{E}\|\|Z$) and A → B ($\vec{E}\perp Z$). Based upon the predictions of crystal field theory we would expect the energy level ordering for the spin-allowed d–d transitions in a tetrahedral d^2 system to be $^3A_2 < {}^3T_2 < {}^3T_1(F) < {}^3T_1(P)$. In C_2 symmetry of course there should be three transitions for every one expected in T_d symmetry. The splitting of the $^3T_1$ states should not be great, however, as the deviation of the PO_4^{3-} tetrahedron in Ca_2PO_4Cl, and presumably the VO_4^{3-} tetrahedron in Sr_2VO_4Cl, from regular tetrahedral symmetry is not large.

Turning now to the spectrum of $Sr_2(VO_4,MnO_4)Cl$, Figure 1, we note the presence of a broad weak absorption band with some attendant fine structure in the 9,000–11,000-cm^{-1} region. This band is present in both polarizations although weaker and with less obvious fine structure when $\vec{E}\perp Z$. This polarization behavior and the attendant weakness of the band strongly support its assignment as the first d–d transition $t_1^6e^2t_2^0 \rightarrow t_1^6et_2^1$ ($^3A_2 \rightarrow {}^3T_2$) as noted above. The

stronger band which occurs with $\vec{E}\|Z$ would then be the A → A component while two A → B transitions would contribute to the weaker band. The same type of treatment may be applied to the band at ~13,000 cm^{-1}; however, trouble is encountered when we attempt to discuss the maximum at ~18,000 cm^{-1}. We observe no band with $\vec{E}\|Z$ (A → A) as we would expect. Relief is obtained from this dilemma by noting that Banks, *et al.*,[2] found that their esr data on $Ca_2(CrO_4,PO_4)Cl$ could be interpreted in terms of D_{2d} molecular symmetry. If this is taken to be the symmetry here, we have the following states present

T_d	D_{2d}
$^3A_2$	$^3B_1$
$^3T_2$	$^3B_2 + {}^3E$
$^3T_1$	$^3A_2 + {}^3E$

The selection rules which apply are $^3B_1 \rightarrow {}^3E$ ($\vec{E}\perp Z$), $^3B_1 \not\rightarrow {}^3B_2$, $^3B_1 \rightarrow {}^3A_2$ ($\vec{E}\|Z$).

Turning our attention to the broad band at 9000–11,000 cm^{-1} and remembering that the lowest d–d transition ($^3A_2 \rightarrow {}^3T_2$ in T_d symmetry) should exhibit a maximum in the $\vec{E}\perp Z$ direction only ($^3B_1 \rightarrow {}^3E$ in D_{2d} symmetry) we note that maxima are present in both polarizations. This would suggest that this absorption band has $^3T_1$ parentage as opposed to $^3T_2$ parentage. This is highly unpalatable as it would produce a reversal of the normal energy ordering. An alternative suggestion is that the parent state is $^3T_2$ but that the transition which occurs with $\vec{E}\|Z$ is vibronically assisted. This would seem logical as there is prominent vibrational structure on this band in the $\vec{E}\|Z$ polarization. This suggestion can be supported as follows. The vibrational progression which appears has a frequency of ~375 cm^{-1}. This indicates that it is the ν_4 bending mode which has also been observed in the spectrum of MnO_4^{2-} [14,15] and CrO_4^{3-}.[3,4] This mode, which belongs to the T_2 representation in T_d symmetry, consists of a B_2 and an E vibration. The electronic transition in which we are interested is $^3B_1 \rightarrow {}^3B_2$. Therefore the products $\Gamma_{elec}\Gamma_z\Gamma_{elec}'\Gamma_{vib}$ for the E and B_2 vibrations are E and A_2 eliminating the possibility of vibrational assistance for this transition. However, if we perform the same operation on the $^3B_1 \rightarrow {}^3E$ transition, we arrive at the products A_1, A_2, B_1, B_2, and E thereby indicating that the $^3B_1 \rightarrow {}^3E$ transition may be vibronically allowed in the $\vec{E}\|Z$ direction. The higher energy band at ~13,000 cm^{-1} exhibits maxima in both polarizations and thus must also have T_1 parentage while that occurring at ~18,000 is present only with $\vec{E}\perp Z$, indicating that it has T_2 parentage. The presence of the ν_4 vibration on these maxima might suggest that these are also d–d transitions. This would require that the first spin-allowed charge-transfer transition occurs at ~32,000 cm^{-1}. Since the first electron-transfer transition occurs at ~18,000 cm^{-1} in MnO_4^- [16] and ~13,000 cm^{-1} in MnO_4^{2-},[17] it would be unlikely that it would occur at an energy as high as 32,000 cm^{-1}. There is also a large difference in intensity between the first absorption band and the higher energy manifolds. We therefore prefer to suggest that these more intense maxima originate from charge-transfer processes with the remaining d–d transitions buried under them.

It should be noted here that the observation of ν_4 on maxima which arise from such a diversity of origins tends to contradict the suggestion of Day, *et al.*,[15] that this vibration is connected to a Jahn–Teller distortion although it is true that the observation of this mode suggests a rather unusual excited-state potential energy surface.

As noted earlier certain maxima in the 9000–11,000-cm^{-1} region appear to be connected by a vibrational frequency of ~400 cm^{-1}. There are, however, other maxima which are present which appear to have no logical connection to the various origins. In addition, lack of resolution in the higher energy members of the progressions adds to the confusion. Therefore, only those bands which are clearly connected are so indicated in Table II.

In Table III it is clear that we are dealing not only with a component of ν_4 vibrational mode but also with the totally symmetric ν_1 and several lattice modes.

The Optical Spectrum of $Li_3(PO_4,MnO_4)$.—Assignment of the spectrum of MnO_4^{3-} in Li_3PO_4 is predicated upon the assumption that the MnO_4^{3-} oxyanion possesses a regular tetrahedral configuration in this host. Support for this assumption is garnered from observations that (1) the PO_4^{3-} species in Li_3PO_4 is a regular tetrahedron, (2) no distortion due to electronic effects would be expected (*e.g.*, tetrahedral d^2 ions should not display a ground-state Jahn–Teller effect, and (3) no polarization behavior is observed (a distortion could be randomly canceling out any overall anisotropic behavior but little can be done optically in this system to substantiate or disprove the existence of such a phenomenon).

Inspection of Figure 2 strongly suggests the presence of two bands comprising the manifold which extends from 10,000 to 20,000 cm^{-1}.

In T_d symmetry the only electronically allowed transitions are $^3A_2 \rightarrow {}^3T_1$. Transitions of the type $^3A_2 \rightarrow {}^3T_2$ may become allowed however by virtue of vibronic coupling. Based upon our earlier result for $Sr_2(VO_4,MnO_4)Cl$, we suggest that the weak band commencing at ~10,000 cm^{-1} corresponds to the $^3A_2$ $(t_1^6e^2) \rightarrow {}^3T_2(t_1^6e^1t_2^1)$ transition and the maximum centered at ~16,000 cm^{-1} with its ~800-cm^{-1} vibrational progression is the $^3A_2(t_1^6e^2) \rightarrow {}^3T_1(t_1^5e^3)$ transition with the $^3A_2(t_1^6e^2) \rightarrow {}^3T_1(t_1^6e^1t_2^1)$ maximum enclosed in this manifold. The maximum at 33,000 cm^{-1} is most likely then the $^3A_2(t_1^6e^2) \rightarrow {}^3T_1(t_1^5e^2t_2^1)$ transition.

Finally, we note the absence of spin-forbidden bands. In the purely tetrahedral case, the transitions $^3A_2 \rightarrow {}^1E$, $^3A_2 \rightarrow {}^1A_1$, and $^3A_2 \rightarrow {}^1T_2$ are both spin and Laporte forbidden. Thus these transitions are simply not observable under the present conditions.

The Electron Spin Resonance Spectrum of $Ca_2(PO_4,MnO_4)Cl$.—The literature dealing with experimental esr results for d^2 systems is quite meager.[18,19] For octahedral complexes the zero-field splitting for d^2

(14) C. A. Kosky and S. L. Holt, *J. Chem. Soc. D*, **11**, 668 (1970).
(15) P. Day, L. Di Sipio, and L. Oleari, *Chem. Phys. Lett.*, **5**, 533 (1970).
(16) S. L. Holt and C. J. Ballhausen, *Theoret. Chim. Acta*, **7**, 313 (1967).
(17) C. A. Kosky, B. R. McGarvey, and S. L. Holt, *J. Chem. Phys.*, in press.
(18) B. R. McGarvey, *Transition Metal Chem.*, **3**, 89 (1966), and references therein.
(19) A Carrington and A. D. McLachlan, "Introduction to Magnetic Resonance," Harper and Row, New York, N. Y., 1967.

ions is usually several reciprocal centimeters in magnitude and the only way in which commonly allowed $\Delta M_s = \pm 1$ transitions become accessible is through the use of pulsed magnets to obtain exceedingly high field densities.[20] On the other hand, the forbidden $\Delta M_s = \pm 2$ transitions have occasionally been seen at cryogenic temperatures.[21-24] Indeed, Schwartz and Carlin[24] have observed patterns which are very similar to those reported here, in guanidinium aluminum sulfate hexahydrate (GASH) doped with V(III). In tetrahedral complexes the zero-field splitting is expected to be smaller but a value of 1.13 cm^{-1} for V^{3+} in CdS has been reported.[25]

The esr results reported here can only be explained as arising from an $S = 1$ system with large zero-field splitting ($D > 1$ cm^{-1}). The 6-line patterns which have been observed in this work must be ascribed to the $\Delta M_s = \pm 2$ transitions for manganese ions in two nonequivalent magnetic sites. The weaker 5-line structures are interpretable as the $\Delta M_s = \pm 1$ transitions.

Although the quality of our esr spectra is not as good as one might like and a more detailed analysis is not possible given the data obtained, one must conclude that a spin-free d^2 system is present.

The Electronic Structure of CrO_4^{3-}. The Optical Spectra of $Ca_2(VO_4,CrO_4)Cl$ and $Sr_2(VO_4,CrO_4)Cl$.—The assignment of the bulk spectra of CrO_4^{3-} in the two vanadate hosts is in agreement with earlier assignments of the spectrum of CrO_4^{3-} in Ca_2PO_4Cl; *i.e.*, the manifolds at 10,000, 17,000, and 27,000 cm^{-1} correspond, respectively, to the low-symmetry components of the $^2E(t_1^6e^1) \rightarrow {}^2T_2(t_1^6e^0t_2^1)$, $^2T_1(t_1^52e^2)$, and $^2T_2(t_1^52e^2)$ transitions. Additional support for the assignment of the 17,000-cm^{-1} maximum to a charge-transfer transition is obtained from the observation of a series of weak maxima superimposed on this band. The two most prominent components of this "progression" occur at 15,400 and 14,650 cm^{-1} and are separated by ~750 cm^{-1}. Progressions of this frequency have been found to be associated with various charge-transfer bands in all oxyanions thus far studied[3,4,6,16,17] but do not appear to accompany the d–d transitions.

The structure superimposed upon the lowest energy transitions is much more complex for $[CrO_3]^{3-}$–$[VO_4]^{3-}$ than for $[CrO_4]^{3-}$–$[PO_4]^{3-}$, however. Referring to Table V and Figure 3, we note that for the polarization parallel to Z we observe a regular progression of about 400-cm^{-1} spacing on the lines at 9950, 10,352, 10,752, and 11,160 cm^{-1}. We also note a progression having roughly 100-cm^{-1} spacing with the 9825-cm^{-1} line as its origin with a component at, or under, the 9950-cm^{-1} line and at 10,050 and 10,152 cm^{-1}. Both the 10,352- and the 10,752-cm^{-1} lines seem to have weak shoulders at about 100 cm^{-1} to higher energy also. The 100-cm^{-1} mode is probably a lattice mode, while the 400-cm^{-1} mode may be related to the $\nu_4(T_2)$ fundamental, which has been reported to be about 410 cm^{-1}.

The assignment of the lines in the polarization having $\vec{E}$ perpendicular to Z is not so straightforward. Here again we see a progression of approximately 400 cm^{-1} built on the line at 9810 cm^{-1}, with components at 10,183 (373), 10,600 (417), and 10,989 (389) cm^{-1}, the splittings given in parentheses. In addition, there seems to be a progression of about 80-cm^{-1} spacing built on the 9810-cm^{-1} line, with components at about 9900, 9970, 10,040, and 10,131 cm^{-1}, and one such component on the high-energy side of the 10,600-cm^{-1} line at 10,672 cm^{-1}. The very weak line at 9660 cm^{-1} does not seem related to any other feature, and the component of moderate size at 10,526 cm^{-1} can only be explained if the line at 10,600 cm^{-1} acts not as the basis transition for the low-energy mode but as the 0–1 component, with the 10,526-cm^{-1} line as the 0–0 transition, which seems highly unlikely. Here as before, we have an active vibration of about 400 cm^{-1}, which again seems to be the $\nu_4(T_2)$ fundamental of CrO_4^{3-}, and a lattice mode at about 80 cm^{-1}.

$Li_3(PO_4,CrO_4)$.—Considering that the host in this instance has tetrahedral symmetry at the phosphate site and that the spectrum of MnO_4^{3-} in this host shows no polarization effects, the obvious, although slight, polarization effects, Figure 4, observed here are undoubtedly associated with a Jahn–Teller distortion. Indeed, one expects a d^1 but not a d^2 system in tetrahedral symmetry to be a Jahn–Teller[26] active system in its ground state.

It should also be noted that in the spodiosite analogs, where the tetrahedral symmetry of the CrO_4^{3-} ion is lowered by virtue of crystal-packing forces (how else is one to explain the distortion of the phosphate, vanadate, or arsenate tetrahedra,[9,12] which can have no Jahn–Teller distortion, in these systems?), no static or dynamic Jahn–Teller effect should be operative, considering that the true symmetry (C_2) or the apparent spectroscopic symmetry (D_{2d}) has nondegenerate electronic ground states. Whether or not a dynamic (vibrational) Jahn–Teller effect may be observable for certain excited states in both the CrO_4^{3-}- and MnO_4^{3-}-doped spodiosite is not easily resolved.

The fact that one axis acts in a unique manner in $Li_3(PO_4,CrO_4)$ must mean that the Jahn–Teller distortion is a concerted one, in which all the dopant ions act in the same geometrical fashion, with specific distortional components appearing only in the xy plane and/or the Z axial directions.

Let us attempt to discover what possible normal vibrational modes may allow such a result. By the argument of Jahn and Teller, the reducible representation of the symmetry group of the displaced configuration which is spanned by integrands of the type $\Phi_\rho^* V_\tau \Phi_\sigma$, where the Φ's are members of a complete set of orthogonal degenerate wave functions, and V_τ is a potential energy operator corresponding to a nuclear configuration displacement from the initial symmetry, must contain the totally symmetric representation, or else the integrals of these integrands vanish. These authors note that Wigner[27] has shown that the normal displacements of the system (which are considered as infinitesimals) may be chosen so that the V_τ transform as irreducible representations of the symmetry group.

(20) S. Foner and W. Low, *Phys. Rev.*, **120**, 1585 (1960).
(21) G. M. Zverev and A. M. Prokhorov, *Zh. Eksp. Teor. Fiz.*, **34**, 1023 (1958); **38**, 449 (1960); **40**, 1016 (1961).
(22) J. Lambe and C. Kituchi, *Phys. Rev.*, **118**, 71 (1960).
(23) R. Y. Hoskins and R. Y. Soffer, *Phys. Rev. A*, **133**, 490 (1964).
(24) R. W. Schwartz and R. L. Carlin, *J. Amer. Chem. Soc.*, **92**, 6763 (1970).
(25) F. S. Hann and G. W. Ludwig, "Paramagnetic Resonance," Vol. 1, W. Low, Ed., Academic Press, New York, N. Y., 1963, p 130.
(26) H. A. Jahn and E. Teller, *Proc. Roy. Soc., Ser. A*, **161**, 220 (1937).
(27) E. Wigner, *Nachr. Ges. Wiss. Goettingen, Math.-Phys. Kl.*, 133 (1930).

Now, where the representations of the wave functions may be chosen as real matrices (as in the present case), then the wave functions also will be real; hence the integrand $\Phi_\rho^* V_\tau \Phi_\sigma$ is equal to $\Phi_\rho \Phi_\sigma V_\tau$ and the set of representations of these transforms as the direct product representation $V_\tau[\Phi^2]$, where $[\Phi^2]$ denotes the symmetric portion of the direct product of Φ with itself. One must note that the set of totally symmetric vibrations, such that $V_\tau = \Gamma_1$, the totally symmetric representation, cannot be Jahn–Teller active. Such vibrations do not change the symmetry of the molecule but simply the internuclear distances. Since the ion or molecule in question is removed from its equilibrium position by such an occurrence but still retains what orbitally degenerate states it had at equilibrium, although at higher total electronic energy, we conclude that any totally symmetric vibrational mode leads to an even less stable condition than the unperturbed equilibrium condition. Thus we are limited to only those vibrational modes which are nontotally symmetric.

We note that in the group T_d the vibrations to be considered correspond to normal coordinates whose irreducible representations are A_1, E, and T_2 (twice) and that the symmetrical portions of the direct products of $E \times E$ and $T_2 \times T_2$ are, respectively, $A_1 + E$ and $A_1 + E + T_2$.

In the present case, the wave functions which are involved in the ground-state Jahn–Teller distortion are the e orbitals. Hence, the only vibrational mode V_τ, which may be active to break up the degeneracy here, is one of symmetry E, as $V_\tau[E^2]$ gives A_1 for E only, in the set $V_\tau = (A_1, E, T_2)$ of the normal modes under consideration. Now the two E normal modes are such that one tends to elongate the tetrahedron along one orthogonal axis while compressing it along the other two, while the second may be described as a "torsional" mode of vibration. Considering the structure of Li_3PO_4, it becomes apparent that the first vibrational mode referred to above will lead to a net elongation of the Cr–O bonds along the crystallographic c axis, by virtue of the disposition of the phosphate tetrahedral sites and the random orientation of the normal coordinates about each such tetrahedron relative to any of the others.

The "torsional" vibrational mode would seem not to affect the "time-average" symmetry of the CrO_4^{3-} ions, on grounds of symmetry. However, it is required by the mathematical argument given above, as only a doubly degenerate nontotally symmetric vibration is sufficient here to break the ground orbital degeneracy.

Although the dynamic Jahn–Teller distortion here seems, statistically, to reduce the symmetry of the CrO_4^{3-} ion to C_{3v} in the ground state, the spectrum of $Li_3(PO_4,CrO_4)$ appears to be interpretable in symmetry T_d, provided we keep in mind the fact that vibrational modes of symmetry E are active here. This is the case because the individual ions are not of symmetry C_{3v} but rather something more of the order of T_d or D_{2d} with their principal axes tipped with regard to the crystallographic axes by about 45°. Thus the radiation is interacting with ions which are nearly tetrahedral individually but which have a time-average symmetry of C_{3v}. Returning to Figure 4, we observe bands in both polarizations (crystallographic a and c) in the region 11,000–16,000 cm^{-1}, bands centered at about 27,000 and 35,000 cm^{-1} in the polarization parallel to c, and bands centered at about 28,000 and 34,000 cm^{-1} in the polarization parallel to a.

We ascribe these bands to transitions as follows: the bands at 11,000–16,000 cm^{-1} seem to be composed of more than a single transition, considering their breadth and the vibrational structure that they show. It is not illogical to suspect that in the present case we are observing the transitions $^2E(t_1^6e^1t_2^0) \rightarrow {}^2T_2(t_1^62e^0t_2^1)$ at about 11,500 cm^{-1} and $^2E \rightarrow {}^2T_1(t_1^52e^2t_2^0)$ at about 13,900 cm^{-1} with associated vibronic interaction of about 700-cm^{-1} spacing, which is somewhat stronger in the polarization parallel to c. The bands at 27,000 and 28,000 cm^{-1} are undoubtedly associated with only one transition, namely, $^2E \rightarrow {}^2T_2(t_1^5e^2t_2^0)$, with an obvious vibrational structure of about 775 cm^{-1} occurring with each band.

It is interesting to note that both of these manifolds have the polarization parallel to c occurring at slightly lower energy than that parallel to a (or b), which tends to confirm the suggestion that an elongation relative to the crystallographic c axis has occurred.

Finally, the featureless bands at 35,000–36,000 cm^{-1} in the two polarizations would seem to be charge transfer in origin, by the arguments given earlier.

Acknowledgment.—The authors wish to thank the NSF and the Research Corp. for support of this work.